The Promotion of Gonadal Cell Divisions by the *Caenorhabditis elegans* TRPM Cation Channel GON-2 Is Antagonized by GEM-4 Copine

Diane L. Church and Eric J. Lambie[1]

Department of Biological Sciences, Dartmouth College, Hanover, New Hampshire 03755

Manuscript received January 11, 2003
Accepted for publication February 6, 2003

ABSTRACT

The initiation of postembryonic cell divisions by the gonadal precursors of *C. elegans* requires the activity of *gon-2*. *gon-2* encodes a predicted cation channel (GON-2) of the TRPM subfamily of TRP proteins and is likely to mediate the influx of Ca^{2+} and/or Mg^{2+}. We report here that mutations in *gem-4* (*gon-2 e*xtragenic *m*odifier) are capable of suppressing loss-of-function alleles of *gon-2*. *gem-4* encodes a member of the copine family of Ca^{2+}-dependent phosphatidylserine binding proteins. Overall, our data indicate that GEM-4 antagonizes GON-2. This antagonism could be mediated by a direct inhibition of GON-2 by GEM-4, since both proteins are predicted to be localized to the plasma membrane. Alternatively, GEM-4 could affect GON-2 activity levels by either promoting endocytosis or inhibiting exocytosis of vesicles that carry GON-2. It is also possible that GEM-4 and GON-2 act in parallel to each other. Mutation of *gem-4* does not suppress the gonadal defects produced by inactivation of *gon-4*, suggesting that *gon-4* either acts downstream of *gem-4* and *gon-2* or acts in a parallel regulatory pathway.

THE gonad of the nematode *Caenorhabditis elegans* is derived from four postembryonic blast cells that initiate divisions several hours after the larva hatches from the egg (Kimble and Hirsh 1979). These divisions require the activity of GON-2, a predicted cation channel of the TRPM (M for melastatin) subfamily of TRP proteins (Duncan *et al.* 1998; West *et al.* 2001; Montell *et al.* 2002b), the founding member of this subgroup.

TRPM proteins are similar to other TRPs in that they have a cluster of six plasma-membrane-spanning segments; however, unlike other TRP proteins, TRPMs have a relatively large C-terminal cytoplasmic domain and lack ankyrin repeats in the N-terminal cytoplasmic domain (Montell *et al.* 2002a). The C-terminal portion of TRPM2 has an ADP-ribose pyrophosphatase domain (Perraud *et al.* 2001) and the C-terminal cytoplasmic segment of TRPM7 has a protein kinase domain (Nadler *et al.* 2001; Runnels *et al.* 2001). Other TRPM channels, *e.g.*, GON-2 and melastatin, have no apparent enzymatic domains. Some TRPM channels function as nonselective cation channels, whereas others are relatively selective for divalent cations (Montell *et al.* 2002a). In addition to Ca^{2+}, certain TRPM channels are also permeable to other physiologically important divalent cations, such as Mg^{2+}, Zn^{2+}, Mn^{2+}, and Co^{2+} (Nadler *et al.* 2001; Schlingmann *et al.* 2002; Walder *et al.* 2002; Monteilh-Zoller *et al.* 2003). The activity of different TRPM channels may be regulated by diverse factors, including phosphorylation (Runnels *et al.* 2001), Mg^{2+}-ATP (Nadler *et al.* 2001), Ca^{2+} (McHugh *et al.* 2003), cold temperature (Peier *et al.* 2002), ADP-ribose (Perraud *et al.* 2001), and cellular redox state (Heiner *et al.* 2003). In the case of melastatin, the channel is constitutively active and may be regulated at the level of translocation to the plasma membrane (Xu *et al.* 2001). TRPM channel activity can affect a range of different cellular functions, depending on channel identity and cell type. Most notably with respect to this study, inactivation of TRPM7 in tissue culture cells leads to growth arrest and cell death (Nadler *et al.* 2001).

It is not known how GON-2 activity is regulated or how its activity regulates the divisions of the gonadal precursor cells. We previously found that *gon-2* mRNA is not restricted to the gonad; however, we were not able to determine whether *gon-2* is expressed within the somatic gonadal cells (West *et al.* 2001). Our working model is that GON-2 is expressed within the gonadal precursors and that it responds to developmental signals by allowing the influx of divalent cations, most likely Ca^{2+} and Mg^{2+} (Nadler *et al.* 2001; Schlingmann *et al.* 2002; Walder *et al.* 2002), which then promote cell cycle progression (Takuwa *et al.* 1995; Wolf and Cittadini 1999).

To identify potential regulators of *gon-2*, we performed a screen for extragenic modifiers of the temperature-sensitive allele, *gon-2(q388)*. One of the genes that we identified in this screen is *gem-4* (*gon-2 e*xtragenic *m*odifier), which encodes a member of the copine family of cytoplasmic, Ca^{2+}-dependent phosphatidylserine binding proteins (Creutz *et al.* 1998; Nakayama *et al.* 1998). Little is known about the biological functions of copines. However, loss-of-function mutations have

[1]*Corresponding author:* 115 Gilman Laboratory, Department of Biological Sciences, Dartmouth College, Hanover, NH 03755.
E-mail: eric.j.lambie@dartmouth.edu

recently been reported for the Arabidopsis copine gene BON1/CPN1 (Hua *et al.* 2001; Jambunathan *et al.* 2001). Mutant plants exhibit cold-sensitive dwarfism due to a combination of reduced cell number and smaller cell size (Hua *et al.* 2001). The basis for this phenotype is not known, although it could result from a defect in vesicle transport or fusion. BON1/CPN1 mutants also exhibit humidity-sensitive precocious cell death and increased pathogen resistance (Jambunathan *et al.* 2001); these abnormalities could result from elevated levels of intracellular calcium.

In this article, we present results indicating that the inactivation of *gem-4* copine can suppress the effects of a reduction in *gon-2* TRPM activity, but cannot suppress the complete inactivation of *gon-2* TRPM. These data suggest that *gem-4(+)* acts as an antagonist of *gon-2(+)*. Such antagonism could be mediated by a direct interaction between the two proteins, or it could be that GON-2 and GEM-4 act in parallel to regulate the divisions of the gonadal precursors.

MATERIALS AND METHODS

Worm culture methods: Nematodes were grown in petri dishes or 12-well microtiter plates using *Escherichia coli* as a food source, essentially as described by Brenner (1974). NGM-lite was used as the growth medium (Sun and Lambie 1997), and *E. coli* strain AMA1004 (Casadaban *et al.* 1993) as the food source.

Microscopy and imaging: Live nematodes were viewed and photographed as described by Sun and Lambie (1997), except that an MTI RC300 CCCD camera was used to integrate images.

Nematode strains: The wild-type N2 background was used in all experiments except the single nucleotide polymorphism (SNP) mapping, which also utilized the wild-type strain CB4856 (Hodgkin and Doniach 1997). Strain construction and genetic analyses were done using standard methods (Sulston and Hodgkin 1988).

The following mutations and rearrangements were used (described by Hodgkin 1997), unless stated otherwise).

Mutations: I: *gon-2(q388)*, *gon-2(dx58)* (West *et al.* 2001), *unc-29(e1072)*; IV: *unc-24(e138)*, *him-8(e1489)*, *dpy-20(e1282)*, *let-60(s1124)*, *let-92(s504)*, *unc-22(s7)*, *unc-31(e169)*.

Chromosomal aberrations: *sDf7 IV* (Moerman and Baillie 1981), *sDf8 IV* (Rogalski *et al.* 1982), *nT1[let-?] IV*; *nT1[deg-3(u662)] V* (referred to here as *DnT1*) (Ferguson and Horvitz 1985; Treinin and Chalfie 1995), *hT2[bli-4(e937)] I; hT2[dpy-18(e364)] III*.

Isolation of mutant alleles of *gem-4*: To identify extragenic modifiers of *gon-2* (specifically, suppressors), we mutagenized hermaphrodites of genotype *gon-2(q388) unc-29(e1072)* and plated them in groups to produce F_1 progeny at permissive temperature. Mutagenesis conditions for UV and EMS was as previously described by Church *et al.* (1995) and Brenner (1974), respectively. The F_1 progeny were expected to include animals of genotype *gem/+* (*gon-2 e*xtragenic *m*odifier) at low frequency. Once the ensuing generation of F_2 progeny began to lay eggs, the plates were shifted to 23.5°. We used 23.5°, because *gon-2(q388)* retains a low level of residual function at this temperature, allowing the possibility of identifying upstream regulators of *gon-2*. At this point in the procedure, some of the F_3 progeny should have progressed beyond the temperature-sensitive period for *gon-2(q388)* (Sun and Lambie 1997), so even if a suppressor mutation were recessive and maternally rescued, some of the *gem/gem* F_3 animals would be expected to be fertile. Plates were permitted to overgrow, and then ~15% of the total progeny were transferred to a new plate, which was again incubated at 23.5°. This procedure was repeated four or five times and then each plate was inspected for the presence of relatively large numbers of fertile animals. Since *q388* is not fully penetrant at 23.5°, even stocks that do not carry suppressor mutations continue to propagate through multiple passages. Therefore, at this point, several fertile individuals were cloned from each plate and tested for their ability to produce a high fraction of non-Gon progeny at 23.5°.

Initial characterization of *gem* mutations: All mutations were outcrossed to *gon-2(q388); him-8(e1489)* males to test for dominance and sex linkage. Subsequent segregation of the *gem* mutation relative to *unc-29(e1072)* and *him-8(e1489)* was used to assess linkage to chromosomes *I* and *IV*, respectively. Four mutations exhibited linkage to *him-8*, and these mutations all fell into the same complementation group, which we designated *gem-4*. Characterization of the other suppressor mutations will be described elsewhere.

Mapping of *gem-4*: We used conventional three-factor mapping to localize *gem-4* on chromosome IV (Figure 1). Among the progeny of hermaphrodites of genotype *gon-2(q388); unc-24(e138) dpy-20(e1282)/gem-4(dx77)*, 0/22 Dpy non-Uncs and 29/29 Unc non-Dpys segregated *gem-4(dx77)*. Therefore, *gem-4* is probably to the right of *dpy-20*. Among progeny of hermaphrodites of genotype *gon-2(q388); let-60(s1124) unc-22(s7) unc-31(e169)/gem-4(dx77)*, 4/6 Unc-22 non-Lets segregated *gem-4 (dx77)*. Therefore, *gem-4* is between *let-60* and *unc-22*.

We identified an SNP within the predicted gene, F38H4.9, and used this to sublocalize *gem-4* within the *let-60-unc-22* interval, as described by Jakubowski and Kornfeld (1999). This was done by constructing a strain of genotype *gon-2(q388); gem-4(dx77) unc-22(s7)/CB4856* and isolating six independent Gem non-Unc progeny. Among the six recombinant chromosomes, two had undergone recombination in the 150-kb interval between *let-60* and F38H4.9 and four had undergone recombination in the 130-kb interval between F38H4.9 and *unc-22* (Figure 1). This placed *gem-4* to the left of F38H4.9 in the vicinity of cosmid T12A7.

Transformation: Standard methods were used to generate and maintain transgenic nematode stocks by coinjection of sample DNAs with plasmid pRF4, which contains the dominant *rol-6(su1006)* marker (Mello *et al.* 1991).

Defecation cycle: Hermaphrodites were raised at 19.5° on uncrowded plates and scored as young adults. Three consecutive defecation cycles were timed for each of five hermaphrodites and standard deviations for each group of animals were calculated using Microsoft Excel.

Plasmid construction: Cosmid T28C1 (which overlaps T12A7, Figure 1) was digested with *Bam*HI and shotgun cloned into pGem7Zf(+) (Promega, Madison, WI), which had been cut with *Bam*HI and dephosphorylated with calf intestinal phosphatase (New England Biolabs, Beverly, MA). PCR was used to identify clones that had the correct insert (an 8574-bp *Bam*HI fragment with 2157 bp upstream of the *gem-4* ATG and 3054 bp downstream of the *gem-4* TAG). There are two *Nde*I cleavage sites in this plasmid (pG41), one of which is ideally situated for creating a C-terminal translational fusion (2 bp upstream of the *gem-4* TAG codon). Therefore, pG41 was partially digested with *Nde*I and linear molecules were isolated by agarose gel electrophoresis, followed by QIAquick (QIAGEN, Chatsworth, CA) purification. Linearized pG41 was ligated with an excess of annealed oligonucleotides o478 (TATCCCGTACGG CGGCCGC) and o479 (TAGCGGCCGC CGTACGGGA). Restriction digests and DNA sequencing were used to identify a plasmid in which the adapter was ligated into

the desired *Nde*I site. The resulting plasmid (pG42) contains unique *Bsi*WI and *Not*I sites immediately upstream of the *gem-4* TAG codon. Primers o481 (AGATCGACGTACGGAGTAAA GGAGAAGAACTTTTC) and o467 (CCCTGCAGGGCGGCC GCCGTACGATGCA) were used to amplify green fluorescent protein (GFP) by PCR, using plasmid L3929 as the template (kindly supplied by A. Fire, Carnegie Institute of Washington). The PCR product was purified using a QIAquick column and digested with *Bsi*WI and *Not*I and ligated into plasmid pG42, cut with the same enzymes. In the resulting plasmid (pG43), the coding sequence for the terminal V of *gem-4* is replaced by PVR, followed by GFP, and then the *gem-4* 3′ flanking sequences.

cDNA isolation: RNA was purified from mixed-stage worms using Trizol (GIBCO/Bethesda Research Laboratories). RT-PCR was performed according to the manufacturer's instructions (Invitrogen, San Diego) to determine the 5′ end and the intron/exon structure of the *gem-4* mRNA. We used PCR to amplify the 3′ end of *gem-4* from a cDNA library kindly supplied by R. Barstead (Barstead and Waterston 1989).

DNA sequencing: PCR was used to amplify ~1-kb segments of *gem-4* genomic DNA, plasmids, or cDNAs for sequencing. These were processed using the BigDye cycle sequencing kit (Applied Biosystems, Foster City, CA) and analyzed by the Dartmouth Molecular Biology Core Facility. Mutant alleles of *gem-4* were sequenced on both strands to confirm their identity.

RNAi experiments: An 850-bp segment of the *gem-4* cDNA was PCR amplified using primers o512 (GCTAATACGAC TCACTATAGGGCTGAACGAGGACGAACTGAA) and o513 (GCTAATACGACTCACTATAGGGTGCAAAGATCCAGGTG TTCG). The first 22 nucleotides (nt) of each primer contains the promoter for T7 RNA polymerase. A 749-bp fragment of genomic DNA corresponding to F26D10.4 was amplified using primers o532 (TAATACGACTCACTATAGGATCCGTGCTA TCCATTTGCC) and o533 (TAATACGACTCACTATAGGCT TCCAGTCCCATCTAGAATC). This segment contains exons of 343 and 350 bp in size. The first 19 nt of each of these primers corresponds to the T7 promoter. A 1456-bp segment of the *gon-2* cDNA was amplified using primers o344 AATA CGACTCACTATACGCGTCGAAGATGTGATTG and o149 AATACGACTCACTATAATCTATGGCATGGTGGTCTT. The first 16 bp of each of these primers contains the T7 promoter. An 873-bp fragment of *gon-4* coding sequence was amplified from genomic DNA using primers o592 TAATACGACTCAC TATAGGCTTAATGGTGGTCTAGAATTG and o591 TAAT ACGACTCACTATAGGCCCGATGAAGCTCAGTACG. The first 19 nt of each of these primers corresponds to the T7 promoter.

The Megascript kit (Ambion, Austin, TX) was used to generate double-stranded RNA (dsRNA) corresponding to *gem-4*, *gon-2*, *gon-4*, and F26D10.4. In each case, ~1 μg of double-strand template DNA was added to the transcription reaction, which was run for ≥7 hr at 37°. Transcription efficiency was monitored by running an aliquot of the reaction on an agarose gel and staining with ethidium bromide. dsRNAs were heated to 60° for ≥10 min, cooled to room temperature, and then injected into the intestine and/or pseudocoelomic cavity of adult hermaphrodites at an estimated concentration of ≥1 μg/μl. Groups of injected animals were incubated on the same plate for at least 8 hr and then transferred to individual plates or multiwells for scoring of offspring.

RESULTS

Identification of *gem-4*: To identify genes that interact with *gon-2*, we screened for revertants of the sterile phenotype of *gon-2(q388)*. These screens resulted in the identification of 25 UV-induced suppressors and 16 EMS-induced suppressors. The total number of genomes screened was ~10^6 for UV and 5.6×10^5 for EMS. However, the efficiency of recovery of suppressor mutations is not likely to be 100%, so the actual frequency of mutations is probably higher than the ~2.5×10^{-5} estimate provided by these data.

Initial outcrosses revealed that four of the mutations (*dx63* and *dx97*, UV; *dx74* and *dx77*, EMS) were recessive and showed linkage to *him-8 IV*. These four mutations represent a single complementation group, which we designated *gem-4*.

Characterization of *gem-4* alleles: Each of the mutant alleles of *gem-4* exhibits a moderately high level of suppression of *gon-2(q388)*, is fully recessive to wild type, and is not maternally rescued (Table 1). We arbitrarily chose *gem-4(dx77)* for most of our further characterization.

Suppression is not specific to *gon-2(q388)*, since *gem-4(dx77)* is also capable of suppressing another missense mutant, *gon-2(dx58)* (Table 2). The efficiency of suppression of *gon-2(dx58)* by *gem-4(dx77)* is similar at 15°, 19.5°,

TABLE 1

Suppression of *gon2(q388)* by mutant alleles of *gen-4*

Genotype	%Gon[a]	*n*
gon-2(q388)	94	386
gon-2(q388); gem-4(dx63)	36	357
gon-2(q388); gem-4(dx74)	45	347
gon-2(q388); gem-4(dx77)	23	265
gon-2(q388); gem-4(dx97)	44	263
gon-2(q388); gem-4(dx63)/+[b]	91	127
gon-2(q388); gem-4(dx74)/+[b]	90	135
gon-2(q388); gem-4(dx77)/+[b]	92	117
gon-2(q388); gem-4(dx77)/sDf7[c]	61	87
gon-2(q388); gem-4(dx77)/sDf8[c]	97	146
gon-2(q388); gem-4(dx77) unc-22(s7); M[gem-4(−)/gem-4(−)][d]	22	167
gon-2(q388); gem-4(dx77) unc-22(s7); M[gem-4(−)/gem-4(+)][e]	26	325

All progeny in these experiments were raised at 23.5°.

[a] Since the gonad is required for induction of the vulva, the absence of the vulva was used to identify animals in which gonadogenesis was severely defective; the majority of these animals had very small gonads (≤50 μm, as assessed by dissecting microscope). In the case of *gem-4*-suppressed animals, ≥90% of the non-Gon animals were fertile. Cell lineaging was not performed on suppressed animals; however, the various tissue subtypes were present and gonad morphology resembled wild type.

[b] Males of genotype *gon-2(q388); him-8(e1489)* were crossed with hermaphrodites of genotype *gon-2(q388) unc-29(e1072); gem-4(−)* and non-Unc F_1 hermaphrodites were scored.

[c] Males of genotype *gon-2(q388); gem-4(dx77)* were crossed with hermaphrodites of genotype *gon-2(q388); DnT1/+ IV; Df/DnT V* and non-Unc F_1 hermaphrodites were scored.

[d] Progeny of a hermaphrodite of genotype *gon-2(q388); gem-4(dx77) unc-22(s7)*.

[e] Progeny of a hermaphrodite of genotype *gon-2(q388); gem-4(dx77) unc-22(s7)/++*.

TABLE 2

Suppression of *gon-2(dx58)* by *gem-4(dx77)*

Genotype	Incubation temperature	%Gon	*n*
gon-2(dx58)	23.5°	87	195
gon-2(dx58); gem-4(dx77)	23.5°	31	297
gon-2(dx58)	19.5°	76	327
gon-2(dx58); gem-4(dx77)	19.5°	24	321
gon-2(dx58)	15°	53	262
gon-2(dx58); gem-4(dx77)	15°	19	512

Groups of gravid hermaphrodites were allowed to lay eggs for several hours at each temperature and then removed. Progeny were scored as adults as in Table 1. All stocks were homozygous for *unc-29(e1072)*. Although *gon-2(dx58)* is temperature sensitive, the ratio of [%Gon among *gon-2(dx58)*]: [%Gon among *gon-2(dx58); gem-4(dx77)*] is very similar at all three temperatures.

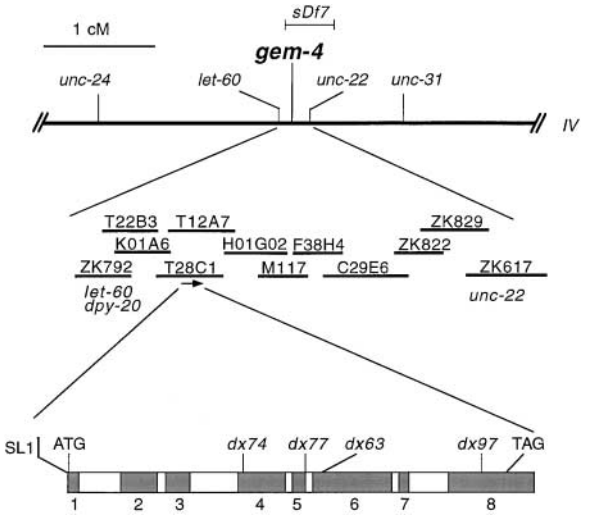

FIGURE 1.—Map location of *gem-4*. (Top) The portion of chromosome *IV* near the *gem-4* locus. Map positions are from the genetic map of *C. elegans* (J. HODGKIN and S. MARTINELLI, personal communication). Cosmids are indicated below the genetic map; positions are based on COULSON (1996) and *C. ELEGANS* SEQUENCING CONSORTIUM (1998). (Bottom) The intron/exon structure of the *gem-4* transcript (exons solid). The 5′ end of the *gem-4* cDNA begins with the SL1 trans-spliced leader sequence, GGTTTAATTACCCAAGTTTGAG, followed by the sequence AAAAAAACACAAAAAATG, where ATG is the initiation codon for *gem-4*. The 3′ end of the *gem-4* cDNA ends with AATAAAGTTTGAACGGG, followed by the poly(A) tail, where AATAAA is the probable cleavage and polyadenylation sequence.

and 23.5°, indicating that *gem-4(dx77)* is not a temperature-sensitive allele.

gem-4(dx77) is capable of suppressing a reduction of *gon-2* activity mediated by RNAi (Table 3). However, the frequency of gonadless (Gon) animals produced by *gon-2(RNAi)* in a wild-type background is lower than that seen in *gon-2(q388)* mutant individuals. This indicates that *gon-2(RNAi)* does not fully eliminate *gon-2(+)* activity. To reduce *gon-2* activity to a negligible level, we performed *gon-2(RNAi)* in a *gon-2(q388)* background at the restrictive temperature for *gon-2(q388)*. In these animals, no suppression by *gem-4(dx77)* was observed. Therefore, suppression by *gem-4(dx77)* requires that the level of *gon-2(+)* activity be above a certain threshold.

sDf7 and *sDf8* are both predicted to remove the *gem-4* locus (MOERMAN and BAILLIE 1981; ROGALSKI *et al.* 1982). We found that *gem-4(dx77)/sDf7* animals exhibit efficient suppression of *gon-2(q388)*, although it is somewhat less than that seen in *gem-4(dx77)* homozygotes. Possibly there is a haplo-insufficient locus within the deleted region that accounts for this difference. No suppression was observed in *gem-4(dx77)/sDf8* animals.

TABLE 3

Effects of *gon-2(RNAi)*

Genotype	%Gon	*n*
N2	0	>500
gon-2(q388)	94	386
N2; *gon-2(RNAi)*	24	388
gem-4(dx77)	0	>500
gem-4(dx77); gon-2 (RNAi)	0.3	754
gon-2(q388); gem-4(dx77)	31	287
gon-2(q388); gem-4(dx77); gon-2 (RNAi)	96	270

Gravid hermaphrodites were allowed to lay eggs at 23.5° and progeny were scored as adults as described in Table 1.

Subsequent PCR analyses using *gem-4*-specific primers revealed that the *gem-4* locus is deleted by *sD7*, but not by *sDf8* (data not shown). Therefore, the *gem-4(dx77)/sDf7* results are consistent with the idea that *gem-4(dx77)* is a loss-of-function allele.

Mapping and cloning *gem-4*: We used a combination of conventional three-factor mapping and SNP mapping to narrow the location of *gem-4* to a position midway between *let-60* and *unc-22* (Figure 1). By assaying cosmids within this interval for their ability to rescue suppression by *gem-4(dx77)*, we determined that *gem-4* is located on cosmid T28C1 (Table 4). The overlapping cosmid, T12A7, contains a predicted gene (T12A7.1) that has two calcium-binding C2 motifs. Since this was a prime candidate for *gem-4*, we sequenced the coding regions of T12A7.1 to search for mutations corresponding to mutant alleles of *gem-4*. In each case, we found a single G → A mutation within the coding region for T12A7.1 (Figure 1; see below). Therefore, we conclude that *gem-4* corresponds to T12A7.1.

We used RT-PCR to amplify and sequence the 5′ end and internal coding region of the *gem-4* transcript. Our results match the intron/exon structure of T12A7.1 described in GenBank. We verified the 3′ end of *gem-4* by PCR amplification and sequencing of cDNA from an oligo(dT)-primed library supplied by R. Barstead (BAR-

TABLE 4

Transgenic rescue of *gem-4(dx77)*

Genotype	%Gon	*n*
gon-2(q388); gem-4(dx77); dxEx11[M117; pRF4]	27	104
gon-2(q388); gem-4(dx77); dxEx9[H01G02; M117; F38H4; C29E6; pRF4]	27	118
gon-2(q388); gem-4(dx77); dxEx12[T28C1; pRF4]	78	185
gon-2(q388); gem-4(dx77); dxEx15[gem-4::GRP; pRF4]	81	160

Gravid hermaphrodites were allowed to lay eggs at 23.5° and progeny were scored as adults as described in Table 1.

STEAD and WATERSTON 1989). It has been suggested that T12A7.1 may be the first gene in an operon consisting of T12A7.1, T12A7.6, and T12A7.7 (BLUMENTHAL *et al.* 2002). T12A7.6 is a novel gene, and T12A7.7 has similarity to G-protein-coupled receptors (WormBase website, http://www.wormbase.org, release WS96, 3/5/03). However, T12A7.6 is trans-spliced to SL1, which is atypical of downstream genes in *C. elegans* operons (WormBase website, http://www.wormbase.org, release WS96, 3/5/03).

***gem-4* encodes a copine:** GEM-4 is highly similar to three human proteins, copine I, copine III, and KIA1599 (>40% identity over ~590 residues; Figure 2). Within the *C. elegans* genome, GEM-4 is most similar to another predicted *C. elegans* gene, F26D10.4 (73% identity over 637 residues). At least three other copine family members, with lower degrees of similarity, are also present in the *C. elegans* genome.

All copines have two ~130-amino-acid (aa) C2 domains in the N-terminal half of the protein (CREUTZ *et al.* 1998; NAKAYAMA *et al.* 1998). C2 domains are found in many different proteins and typically mediate binding to Ca^{2+} (RIZO and SUDHOF 1998). The C-terminal half of copine proteins contains an A domain of ~200 aa that has similarity to the Mg^{2+}-binding domain of integrins (CREUTZ *et al.* 1998; NAKAYAMA *et al.* 1998).

Mutant alleles of *gem-4*: Each of the mutant alleles of *gem-4* that we identified alters the predicted protein coding sequence (Figures 1 and 2). *dx74* and *dx63* alter different glycine residues, each of which is adjacent to a potential serine/threonine phosphorylation site that is conserved among the metazoan relatives of GEM-4 (but absent from Arabidopsis BON1). *dx74* is between the two C2 domains, while *dx63* is near the end of the second C2 domain (C2B). *gem-4(dx77)* alters a splice site upstream of intron 5. We used RT-PCR to examine the splicing pattern in *gem-4(dx77)* animals and found that intron 5 is retained within the resulting mRNA. Since this intron is 45 nt in length and contains no stop codons within the GEM-4 reading frame, *dx77* is predicted to result in a 15-amino-acid insertion, beginning after P286. This insertion is likely to disrupt C2B function. *dx97* causes a E → K substitution in the C-terminal portion of GEM-4, adjacent to the A domain. Although this region is conserved among the various copines, no function has been ascribed to this portion of the protein.

***gem-4::GFP* expression pattern:** To determine when and where *gem-4* is expressed during *C. elegans* development, we fused the coding sequence of GFP to the 3′ end of the coding sequence of GEM-4 and generated transgenic animals carrying this construct. We examined the expression and localization of GEM-4::GFP in three different backgrounds: wild type (N2), *gon-2(q388); gem-4(dx77)*, and *gon-2(q388)*. No obvious differences in expression pattern were observed in these different backgrounds (data not shown).

The *gem-4::GFP* reporter gene complements *gem-4(dx77)* just as efficiently as the cosmid T28C1, suggesting that the fusion protein is expressed and functions within the tissues within which GEM-4 normally acts (Table 4). In cells that express GEM-4::GFP, fluorescence is typically brightest at the plasma membrane. In some cases, punctate staining is also evident within the cytoplasm, possibly due to association with vesicular structures (Figure 3). We have not systematically examined the embryonic expression pattern; however, GEM-4::GFP is broadly expressed in embryos that have several hundred cells and continues to be expressed in most cells as the embryo undergoes elongation (Figure 4).

In newly hatched L1s, GEM-4::GFP is expressed in the precursors of the somatic gonad (Z1 and Z4), the pharyngeal/intestinal valve cells, the intestinal cells, and the head mesodermal cell (the sister of Z4; Figures 4 and 5). The germline precursors, Z2 and Z3, also appear to be outlined in some animals (Figure 5); however, it is not clear whether this is due to expression within the germ cells themselves or whether it results from extensions of the plasma membranes of Z1 and Z4.

Localization of GEM-4::GFP to the plasma membrane is not dependent on *gon-2* activity, since this is not altered at restrictive temperature in animals of background genotype *gon-2(q388); gem-4(dx77)* or *gon-2(q388)* (Figure 5). Expression of GEM-4::GFP within Z1 and Z4 becomes progressively more difficult to detect as the animals progress through L1 and is not detectable within the progeny of Z1 and Z4. GEM-4::GFP expression within somatic gonadal tissues does not resume until early adulthood. At this point, GEM-4::GFP be-

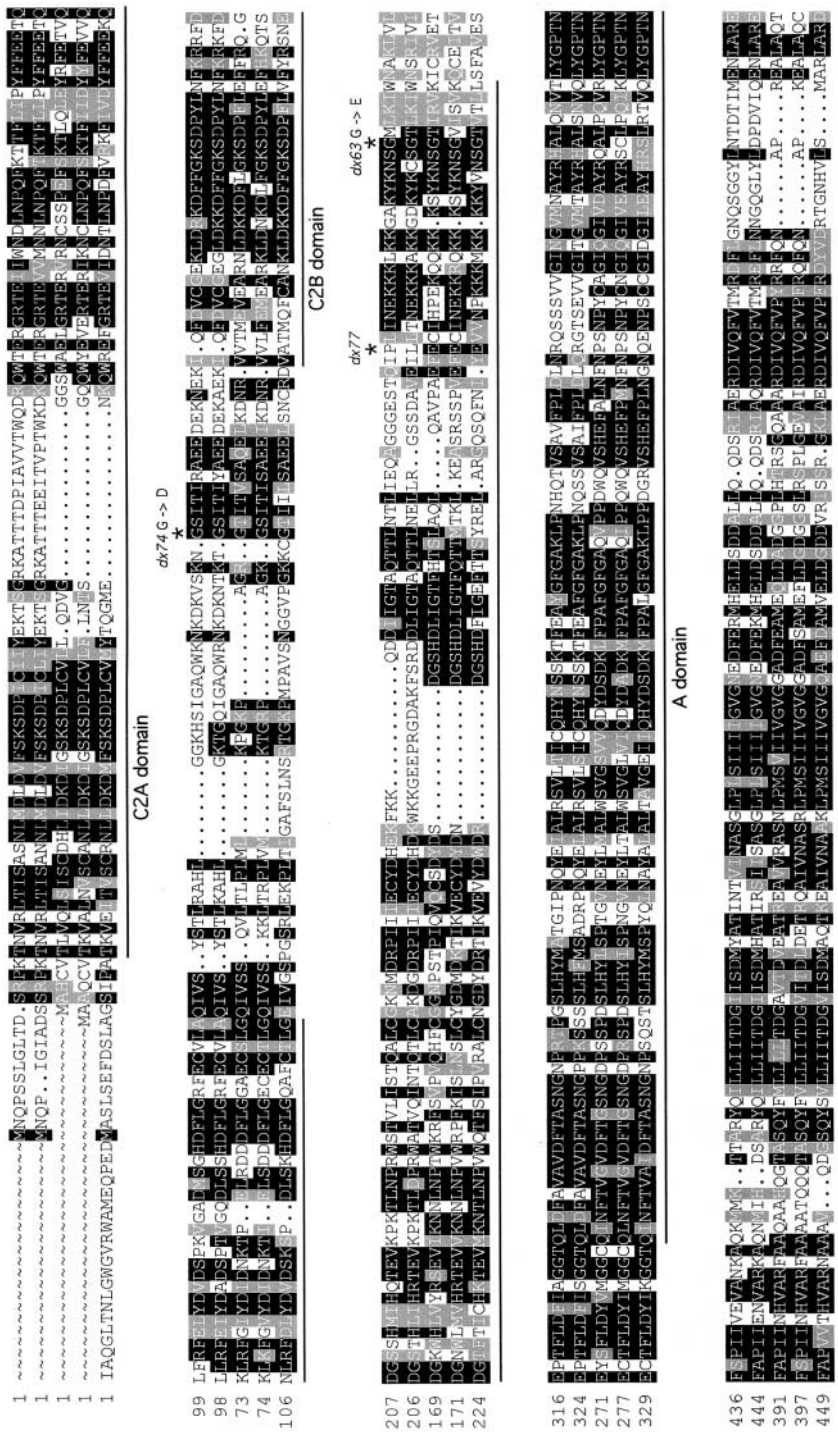

FIGURE 2.—Predicted amino acid sequence of GEM-4 and other copines. Full-length proteins were compared using the PILEUP program of the UWGCG software package. Shading was done using BOXSHADE, with identical residues shaded in black and similar residues in gray. Conserved transmembrane domains S1–S6 are indicated. Residues affected by mutations in *gem-4* are indicated with an asterisk and the nature of the predicted amino acid alteration. *dx77* is predicted to result in the insertion of "TNLKLFSNFKIYNFQ" after proline 286. COP1, human copine I (AAH01142); COP3, human copine III (O75131); KIAA1599 (Q9HCH3); F26D10.4 is also known as T28F3.1 (Q9XUB9); GEM-4 is T12A7.1 (NP_502225).

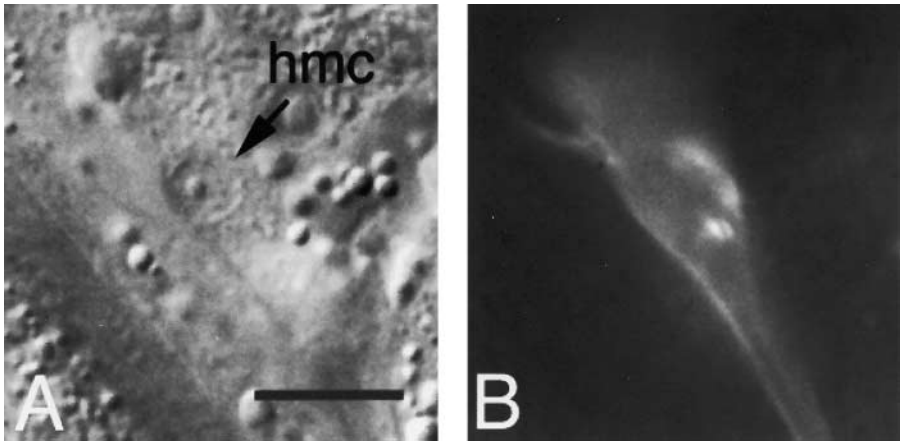

FIGURE 3.—Punctate expression of GEM-4::GFP. (A) Differential interference contrast (DIC) image of the head mesodermal cell (nucleus indicated) in an adult animal of genotype *gon-2(q388); gem-4(dx77); dxEx15[gem-4::GFP; pRF4]*. (B) GFP fluorescence of the same field. GEM-4::GFP outlines the plasma membrane of the head mesodermal cell (hmc) and is also present as multiple discrete puncta (only one is distinct in this focal plane). Bar, ~5 μm.

comes strongly expressed within the distal spermathecal cells, the spermathecal valve cells, and the uterine epithelial cells (Figure 6).

***gem-4(dx77)* and *gem-4(dx74)* have no apparent phenotype in a wild-type background:** We outcrossed *gem-4(dx74)* and *gem-4(dx77)* to determine whether these mutations produce any mutant phenotypes in a *gon-2(+)* background. However, neither strain is obviously different from wild type in terms of growth rate, gonad development, behavior, or dependence of gonadal cell divisions on the availability of food (data not shown). We determined brood sizes among animals raised at either 15° or 23.5°. At 15°, we found that the brood sizes for N2 (mean 265, SD 29, $n = 3$) and *gem-4(dx77)* (mean 240, SD 25, $n = 4$) were similar, whereas that for *gem-4(dx74)* was somewhat lower (mean 162, SD 58, $n = 4$). We obtained similar results for brood sizes at 23.5°: N2, mean 233, SD 65, $n = 4$; *gem-4(dx77)*, mean 253, SD 37, $n = 4$; *gem-4(dx74)*, mean 173, SD 43, $n = 4$. The relatively low fecundity of the *gem-4(dx74)* strain may be due to a mutation in a separate gene that was not removed during outcrossing of the mutagenized stock.

Since *gem-4* is implicated in the regulation of calcium-mediated signaling, and calcium levels within the intestinal cells are known to regulate the defecation cycle (DAL SANTO *et al.* 1999), we compared the periodicity of defecation in *gem-4(dx74)* and *gem-4(dx77)* animals with N2 individuals grown in parallel. Very similar periodicities were observed in each case: N2, 48.9 sec, SD 3.2; *gem-4(dx74)*, 49.8 sec, SD 3.2; *gem-4(dx77)*, 51.0 sec, SD 3.5. We also examined the defecation cycle of animals of genotype *gon-2(q388)* and *gon-2(q388); gem-4(dx77)* and found no apparent difference between these animals and wild-type controls (data not shown).

Inactivation of *gem-4* by RNAi: We used RNAi to determine whether reducing the level of *gem-4* activity is suffi-

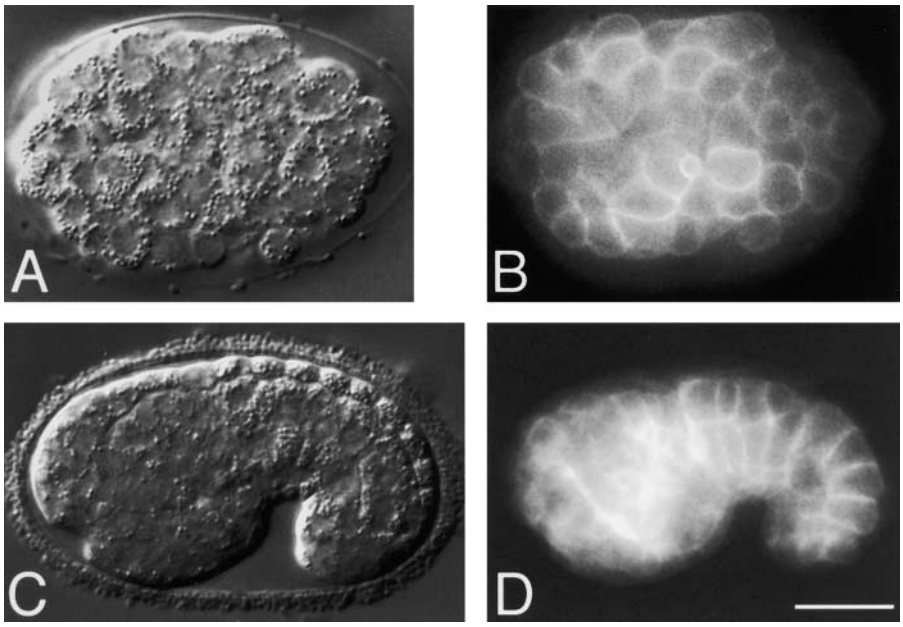

FIGURE 4.—Embryonic expression of GEM-4::GFP. (A and B) Midstage embryo, prior to morphogenesis. (C and D) Comma stage embryo. Both embryos have genotype *gon-2(q388); gem-4(dx77); dxEx15[gem-4::GFP; pRF4]*. DIC is shown in A and C, GFP fluorescence in B and D. Anterior is to the left, dorsal is up (dorsal/ventral not determined in A and B). Bar, ~10 μm.

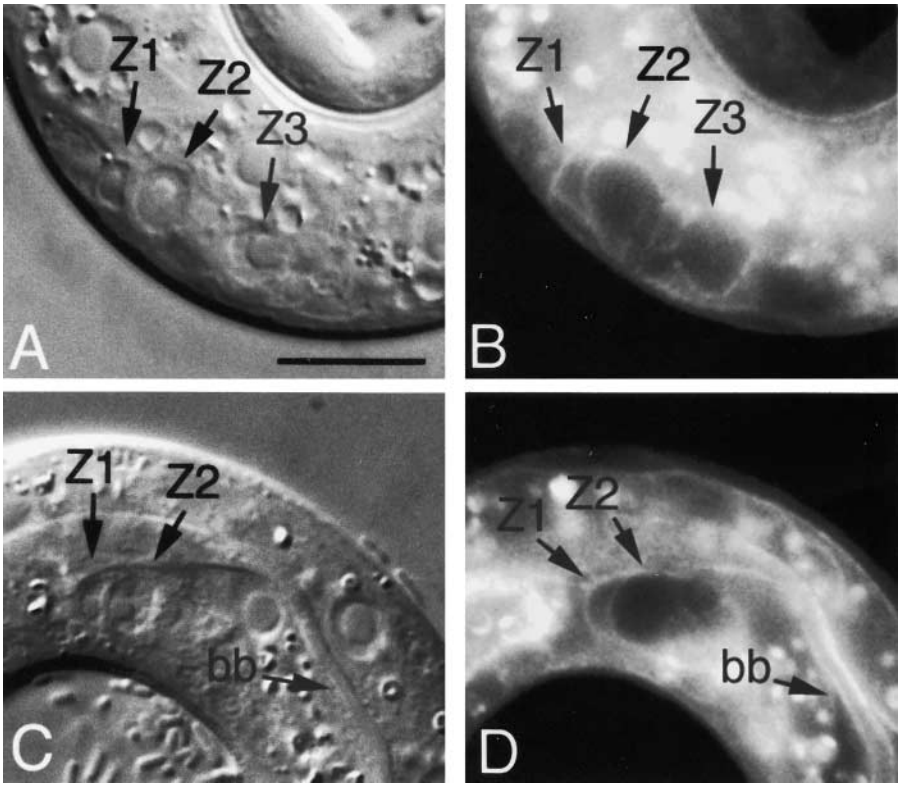

FIGURE 5.—Expression of GEM-4::GFP in L1 larvae. (A and B) DIC and GFP fluorescence images of an early L1 stage animal of genotype *gon-2(q388); gem-4(dx77); dxEx15[gem-4::GFP; pRF4]* raised at 15° [permissive temperature for *gon-2(q388)*]. (C and D) DIC and GFP fluorescence images of an early L1 stage animal of genotype *gon-2(q388); dxEx15 [gem-4::GFP; pRF4]* raised at 25° [restrictive temperature for *gon-2(q388)*]. *gem-4::GFP* is also localized to the intestinal brush border (bb). The granular/globular fluorescence in B and D is due to autofluorescence of gut granules. Bar, ~10 μm.

cient to suppress *gon-2(q388). gem-4(RNAi)* suppresses *gon-2(q388)* nearly as efficiently as the mutant alleles of *gem-4* (Table 5). To assess the efficacy of the RNAi treatment, we also tested animals carrying an extrachromosomal array that contains *gem-4::GFP*. In nearly all of these animals GFP fluorescence was either eliminated or greatly reduced. In addition, the rescuing effects of GEM-4::GFP were severely attenuated by *gem-4(RNAi)* (Table 5).

We also tested whether *gem-4(RNAi)* would enhance the suppression of *gon-2(q388)* by *gem-4(dx77)* or cause a detectable phenotype in animals of genotype *gem-4 (dx77). gem-4(RNAi)* had no discernible effect in either experiment, suggesting that *gem-4(dx77)* is a strong loss-of-function allele (Table 5).

To investigate the possibility that *gem-4* is functionally redundant to F26D10.4, we also examined the effects of F26D10.4(RNAi). F26D10.4(RNAi) weakly suppressed *gon-2(q388)*, but did not alter the penetrance of suppression of *gon-2(q388)* by *gem-4(dx77)* or produce any obvious effects in a wild-type background (Table 6). We suspect that the weak suppressive effect of F26D10.4 (RNAi) may be due to cross-inactivation of *gem-4*, because several ≥30-nt stretches of ~90% identity between *gem-4* and F26D10.4 are present within the region that was used to generate the double-stranded RNA. HUANG *et al.* (2002) have reported that this degree of similarity can be sufficient to cause significant RNAi effects.

***gem-4(dx77)* does not suppress the effects of inactivation of *gon-4*:** The *gon-4* gene encodes a large nuclearly localized protein whose function is important for the initial divisions of the gonadal precursors (FRIEDMAN *et al.* 2000). To investigate the possibility that *gem-4(−)* might be able to suppress the effect of inactivation of *gon-4*, we compared the effects of *gon-4(RNAi)* in *gem-4(+)* and *gem-4(dx77)* genetic backgrounds. We found no evidence of suppression. Among the progeny of injected *gem-4(dx77)* hermaphrodites, 50% ($n = 942$, from 14 injected animals) exhibited gonadal defects typical of *gon-4* inactivation (ranging from vulvaless with little gonadal tissue to Egl), whereas 36% of the progeny of injected *gem-4(+)* hermaphrodites exhibited such defects ($n = 631$, from 7 injected animals). The intermediate penetrance of the Gon-4 phenotypes indicates that *gon-4* activity was not completely eliminated by the RNAi treatment. Therefore, suppression by *gem-4(dx77)* should have been detectable, even if *gem-4(dx77)* cannot suppress *gon-4(0)*. Furthermore, dead eggs and L1 lethal progeny were often observed in the latter part of the broods of injected animals, suggesting that a severe reduction in *gon-4* activity can cause more extreme developmental defects. The absence of embryonic lethals and L1 lethals among the progeny of *gon-4(0)/+* hermaphrodites (FRIEDMAN *et al.* 2000) is probably due to maternal rescue by *gon-4(+)*.

DISCUSSION

In our screen for genes that interact with *gon-2*, we identified four mutant alleles of the *gem-4* locus. Several

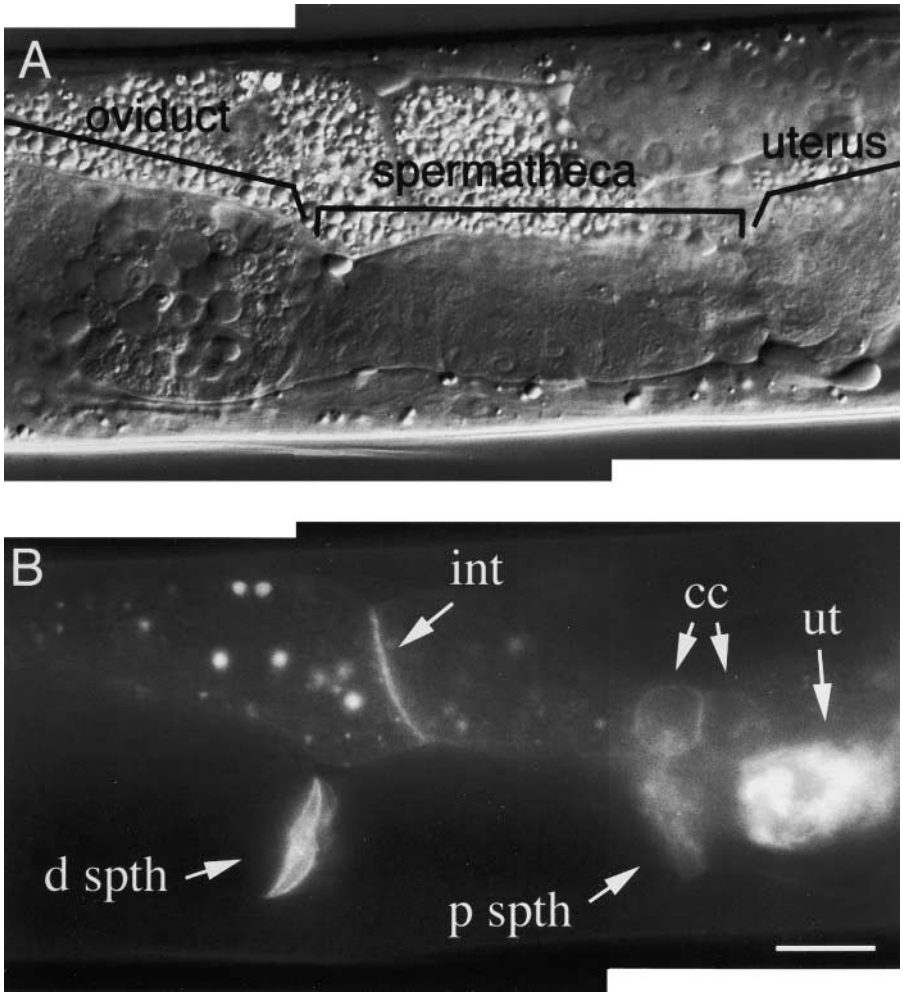

FIGURE 6.—Expression of GEM-4::GFP in late L4. (A and B) DIC and GFP images of a late-L4-stage hermaphrodite of genotype *gon-2(q388); gem-4(dx77); dxEx15[gem-4::GFP; pRF4]*. Expression of GEM-4::GFP is evident within cells of the distal (d) and proximal (p) spermatheca (spth), uterus (ut), intestine (int), and coelomocytes (cc). The punctate fluorescence in the intestine is due to autofluorescent gut granules. Bar, ~10 μm.

lines of evidence suggest that these are strong loss-of-function alleles of *gem-4*. First, each mutant allele is recessive to wild type. Second, *gem-4(dx77)* fails to complement the deficiency, *sDf7*. Third, *gem-4(RNAi)* suppresses *gon-2(q388)* nearly as effectively as the mutant alleles of *gem-4*. Fourth, the degree of suppression of *gon-2(q388)* by *gem-4(dx77)* is not altered when combined with *gem-4(RNAi)*.

TABLE 5

Effects of *gem-4(RNAi)*

Genotype	%Gon	*n*
gon-2(q388)	92	617
gon-2(q388); gem-4(RNAi)	46	552
gon-2(q388); gem-4(dx77)	42	607
gon-2(q388); gem-4(dx77); gem-4(RNAi)	38	531
gon-2(q388); gem-4(dx77); dxEx15[gem-4::GFP; pRF4][a]	66	289
gon-2(q388); gem-4(dx77); dxEx15[gem-4::GFP; pRF4] gem-4(RNAi)[b]	28	145
N2	0	>500
N2; *gem-4(RNAi)*	0	>500

Gravid hermaphrodites were allowed to lay eggs at 23.5° and progeny were scored as adults as described in Table 1.

[a] Among Ro1 animals randomly picked for inspection, 32/34 exhibited strong GEM-4::GFP signal in the gut (and usually in other tissues also).

[b] Among Ro1 animals randomly picked for inspection, 1/34 exhibited strong GEM-4::GFP signal in the gut. A total of 15/34 had no apparent GEM-4::GFP and the others had weak or mosaic expression.

TABLE 6

Effects of F26D10.4(RNAi)

Genotype	%Gon	*n*
N2	0	>300
N2; F26D10.4(RNAi)	0	>300
gen-4(dx77)	0	>300
gem-4(dx77); F26D10.4(RNAi)	0	>300
gon-2(q388)	96	527
gon-2(q388); F26D10.4(RNAi)	79	1071
gon-2(q388); gem-4(dx77)	37	554
gon-2(q388); gem-4(dx77); F26D10.4(RNAi)	34	1028

Gravid hermaphrodites were allowed to lay eggs at 23.5° and progeny were scored as adults as described in Table 1.

gem-4 encodes a member of the copine family of Ca^{2+}-binding proteins (Creutz *et al.* 1998; Nakayama *et al.* 1998). Copines have two C2 domains in the N-terminal portion of the protein that mediate Ca^{2+}-dependent binding to phosphatidylserine-containing membranes (Creutz *et al.* 1998; Tomsig and Creutz 2000). Copines also have an A domain in the C-terminal portion; this region has been proposed to bind Mg^{2+} and may have kinase activity (Caudell *et al.* 2000). Three of our mutant alleles affect the portion of GEM-4 that contains the C2 domains, and the fourth allele is adjacent to the A domain. These results are consistent with the expectation that both of these regions are important for normal copine function.

We found that GEM-4::GFP is constitutively localized to the plasma membrane in all cells that express the fusion protein, regardless of the activity state of *gon-2* (and therefore possibly not dependent on high levels of intracellular calcium). This could be an artifact due to the GFP fusion or an unusually high level of protein expressed from the extrachromosomal array. However, Ca^{2+} is not essential for copines to bind to lipid membranes composed of phosphatidic acid (Tomsig and Creutz 2000) or plasma membranes isolated from Arabidopsis cells (Hua *et al.* 2001). Furthermore, Hua *et al.* (2001) found that a BON1::GFP fusion protein was constitutively localized to the plasma membrane in transfected leaf protoplasts.

Mutation of the Arabidopsis copine gene, BON1/CPN1, causes a cold-sensitive growth defect, suggesting the possibility that copines are generally required for membrane fusion events at relatively low temperatures (Hua *et al.* 2001). Our data do not provide support for this idea in the case of GEM-4, since we found no difference in the degree of suppression of *gon-2(−)* by *gem-4(−)* at different temperatures. Mutations in BON1/CPN1 also cause a hypersensitive stress response that may result from elevated intracellular Ca^{2+} signaling (Jambunathan *et al.* 2001). This is directly comparable to our findings regarding *gon-2* and could conceivably result from an elevation of calcium channel activity in Arabidopsis BON1/CPN1 mutants.

Suppression by *gem-4* requires at least a low level of *gon-2* function. Therefore, *gem-4* does not operate downstream of *gon-2* in a simple linear regulatory pathway. Overall, our results are consistent with a model in which GON-2 and GEM-4 are both expressed and localize to the plasma membrane of the somatic gonad precursors at the beginning of the first larval stage. We hypothesize that GON-2 mediates an influx of mitogenic cations in response to developmental signals produced at the onset of postembryonic development. The resulting increase in free intracellular Ca^{2+} and Mg^{2+} could lead to the activation of GEM-4, which could then negatively regulate GON-2, possibly by direct phosphorylation.

Since copines may potentially be involved in vesicle trafficking (Creutz *et al.* 1998) and some TRP channels may be regulated by the fusion of channel-containing vesicles with the plasma membrane (Kanzaki *et al.* 1999; Xu *et al.* 2001), it is possible that inactivation of *gem-4* suppresses *gon-2(lf)* by increasing the number of GON-2 channels that are present within the plasma membrane. In this scenario, GEM-4 could be either a positive regulator of endocytosis or a negative regulator of the fusion/transport of GON-2-containing vesicles to the plasma membrane.

Our data are also consistent with the possibility that GEM-4 acts in parallel to GON-2 to modulate the level of intracellular Ca^{2+} and/or Mg^{2+} signaling. This could be accomplished by either altering the level of free intracellular cations or affecting the activity of one or more signal transduction components.

gon-4 encodes a novel nuclear protein whose inactivation causes an impairment of gonadal cell divisions similar to that seen in *gon-2* mutants (but slightly less severe; Friedman *et al.* 2000). Given the similarity of their mutant phenotypes, it is possible that a positive regulatory relationship exists between *gon-2* and *gon-4*. In a simple linear pathway, *gon-4* could act either upstream or downstream of *gon-2*. In the first case, inactivation of *gon-4* would cause a reduction in *gon-2* activity, which would then lead to the mutant phenotype. If this model were correct, then *gem-4(lf)* should suppress the effects of inactivation of *gon-4*, since *gem-4(lf)* potentiates *gon-2* activity. We found that *gem-4(lf)* does not suppress the gonadal defects caused by *gon-4(RNAi)*. Therefore, *gon-4* is likely to act either downstream of *gon-2* (and *gem-4*) or as part of a separate regulatory pathway required for the divisions of the gonadal precursors.

We have not observed any obvious defects in the timing or pattern of gonadal divisions when *gem-4* mutations are present in a *gon-2(+)* background. Furthermore, *gon-2(q388)* is not fully suppressed by inactivation of *gem-4*. Together, these results suggest the possibility that *gem-4* may be redundant to one or more other genes. We investigated this possibility by using RNAi to attempt to inactivate the paralogous gene, F26D10.4; however,

this treatment had little or no effect. Perhaps regulation by *gem-4* is merely a fine-tuning mechanism whose disruption has no overt consequences when the expression and function of *gon-2* is normal. This would be consistent with other reports of extragenic suppressor mutations that have little or no obvious phenotype other than their suppressor activity (Maine and Kimble 1993; Jongeward *et al.* 1995; Grant and Greenwald 1996).

We thank Theresa Stiernagle and the Caenorhabditis Genetics Stock Center [which is supported by the National Institutes of Health (NIH) National Center for Research Resources] for many of the strains used in this study, Andy Fire for the L3929 vector, Bob Barstead for the cDNA library, Alan Coulson and the Sanger Center for providing cosmids, Rachel West for ds *gon-2* RNA, Victor Ambros for helpful comments on the manuscript, and reviewers for additional constructive suggestions. This work was supported by NIH grant RO1-GM49785.

LITERATURE CITED

Barstead, R. J., and R. H. Waterston, 1989 The basal component of the nematode dense-body is vinculin. J. Biol. Chem. **264:** 10177–10185.

Blumenthal, T., D. Evans, C. D. Link, A. Guffanti, D. Lawson *et al.*, 2002 A global analysis of *Caenorhabditis elegans* operons. Nature **417:** 851–854.

Brenner, S., 1974 The genetics of *Caenorhabditis elegans*. Genetics **77:** 71–94.

C. elegans Sequencing Consortium, 1998 Genome sequence of the nematode *C. elegans*: a platform for investigating biology. Science **282:** 2012–2018.

Casadaban, M. J., A. Martinez-Arias, S. K. Shapira and J. Chaou, 1993 β-Galactosidase gene fusions for analyzing gene expression in *Escherichia coli* and yeast. Methods Enzymol. **100:** 293–299.

Caudell, E. G., J. J. Caudell, C. H. Tang, T. K. Yu, M. J. Frederick *et al.*, 2000 Characterization of human copine III as a phosphoprotein with associated kinase activity. Biochemistry **39:** 13034–13043.

Church, D. L., K. L. Guan and E. J. Lambie, 1995 Three genes of the MAP kinase cascade, *mek-2*, *mpk-1/sur-1* and *let-60 ras*, are required for meiotic cell cycle progression in *Caenorhabditis elegans*. Development **121:** 2525–2535.

Coulson, A., 1996 The Caenorhabditis elegans genome project. *C. elegans* Genome Consortium. Biochem. Soc. Trans. **24:** 289–291.

Creutz, C. E., J. L. Tomsig, S. L. Snyder, M. C. Gautier, F. Skouri *et al.*, 1998 The copines, a novel class of C2 domain-containing, calcium-dependent, phospholipid-binding proteins conserved from Paramecium to humans. J. Biol. Chem. **273:** 1393–1402.

Dal Santo, P., M. A. Logan, A. D. Chisholm and E. M. Jorgensen, 1999 The inositol trisphosphate receptor regulates a 50-second behavioral rhythm in *C. elegans*. Cell **98:** 757–767.

Duncan, L. M., J. Deeds, J. Hunter, J. Shao, L. M. Holmgren *et al.*, 1998 Down-regulation of the novel gene melastatin correlates with potential for melanoma metastasis. Cancer Res. **58:** 1515–1520.

Ferguson, E. L., and H. R. Horvitz, 1985 Identification and characterization of 22 genes that affect the vulval cell lineages of the nematode *Caenorhabditis elegans*. Genetics **110:** 17–72.

Friedman, L., S. Santa Anna-Arriola, J. Hodgkin and J. Kimble, 2000 *gon-4*, a cell lineage regulator required for gonadogenesis in *Caenorhabditis elegans*. Dev. Biol. **228:** 350–362.

Grant, B., and I. Greenwald, 1996 The *Caenorhabditis elegans sel-1* gene, a negative regulator of *lin-12* and *glp-1*, encodes a predicted extracellular protein. Genetics **143:** 237–247.

Heiner, I., J. Eisfeld, C. R. Halaszovich, E. Wehage, E. Jungling *et al.*, 2003 Expression profile of the transient receptor potential (TRP) family in neutrophil granulocytes: evidence for currents through LTRPC2 induced by ADP-ribose and NAD. Biochem. J. **4:** 4.

Hodgkin, J., 1997 Genetics, pp. 881–1047 in *C. elegans II*, edited by D. Riddle, T. Blumenthal, B. Meyer and J. Priess. Cold Spring Harbor Laboratory Press, Cold Spring Harbor, NY.

Hodgkin, J., and T. Doniach, 1997 Natural variation and copulatory plug formation in *Caenorhabditis elegans*. Genetics **146:** 149–164.

Hua, J., P. Grisafi, S. H. Cheng and G. R. Fink, 2001 Plant growth homeostasis is controlled by the Arabidopsis BON1 and BAP1 genes. Genes Dev. **15:** 2263–2272.

Huang, N. N., D. E. Mootz, A. J. Walhout, M. Vidal and C. P. Hunter, 2002 MEX-3 interacting proteins link cell polarity to asymmetric gene expression in *Caenorhabditis elegans*. Development **129:** 747–759.

Jakubowski, J., and K. Kornfeld, 1999 A local, high-density, single-nucleotide polymorphism map used to clone *Caenorhabditis elegans cdf-1*. Genetics **153:** 743–752.

Jambunathan, N., J. M. Siani and T. W. McNellis, 2001 A humidity-sensitive Arabidopsis copine mutant exhibits precocious cell death and increased disease resistance. Plant Cell **13:** 2225–2240.

Jongeward, G. D., T. R. Clandinin and P. W. Sternberg, 1995 *sli-1*, a negative regulator of *let-23*-mediated signaling in *C. elegans*. Genetics **139:** 1553–1566.

Kanzaki, M., Y. Q. Zhang, H. Mashima, L. Li, H. Shibata *et al.*, 1999 Translocation of a calcium-permeable cation channel induced by insulin-like growth factor-I. Nat. Cell Biol. **1:** 165–170.

Kimble, J., and D. Hirsh, 1979 Post-embryonic cell lineages of the hermaphrodite and male gonads in *C. elegans*. Dev. Biol. **70:** 396–417.

Maine, E. M., and J. Kimble, 1993 Suppressors of *glp-1*, a gene required for cell communication during development in *Caenorhabditis elegans*, define a set of interacting genes. Genetics **135:** 1011–1022.

McHugh, D., R. Flemming, S. Z. Xu, A. L. Perraud and D. J. Beech, 2003 Critical intracellular Ca^{2+} dependence of transient receptor potential melastatin 2 (TRPM2) cation channel activation. J. Biol. Chem. **278:** 11002–11006.

Mello, C. C., J. M. Kramer, D. Stinchcomb and V. Ambros, 1991 Efficient gene transfer in *C. elegans*: extrachromosomal maintenance and integration of transforming sequences. EMBO J. **10:** 3959–3970.

Moerman, D. G., and D. L. Baillie, 1981 Formaldehyde mutagenesis in the nematode *Caenorhabditis elegans*. Mutat. Res. **80:** 273–279.

Monteilh-Zoller, M. K., M. C. Hermosura, M. J. Nadler, A. M. Scharenberg, R. Penner *et al.*, 2003 TRPM7 provides an ion channel mechanism for cellular entry of trace metal ions. J. Gen. Physiol. **121:** 49–60.

Montell, C., L. Birnbaumer and V. Flockerzi, 2002a The TRP channels, a remarkably functional family. Cell **108:** 595–598.

Montell, C., L. Birnbaumer, V. Flockerzi, R. J. Bindels, E. A. Bruford *et al.*, 2002b A unified nomenclature for the superfamily of TRP cation channels. Mol. Cell **9:** 229–231.

Nadler, M. J., M. C. Hermosura, K. Inabe, A. L. Perraud, Q. Zhu *et al.*, 2001 LTRPC7 is a Mg.ATP-regulated divalent cation channel required for cell viability. Nature **411:** 590–595.

Nakayama, T., T. Yaoi, M. Yasui and G. Kuwajima, 1998 N-copine: a novel two C2-domain-containing protein with neuronal activity-regulated expression. FEBS Lett. **428:** 80–84.

Peier, A. M., A. Moqrich, A. C. Hergarden, A. J. Reeve, D. A. Andersson *et al.*, 2002 A TRP channel that senses cold stimuli and menthol. Cell **108:** 705–715.

Perraud, A. L., A. Fleig, C. A. Dunn, L. A. Bagley, P. Launay *et al.*, 2001 ADP-ribose gating of the calcium-permeable LTRPC2 channel revealed by Nudix motif homology. Nature **411:** 595–599.

Rizo, J., and T. C. Sudhof, 1998 C2-domains, structure and function of a universal Ca^{2+}-binding domain. J. Biol. Chem. **273:** 15879–15882.

Rogalski, T. M., D. G. Moerman and D. L. Baillie, 1982 Essential genes and deficiencies in the *unc-22* IV region of *Caenorhabditis elegans*. Genetics **102:** 725–736.

Runnels, L. W., L. Yue and D. E. Clapham, 2001 TRP-PLIK, a bifunctional protein with kinase and ion channel activities. Science **291:** 1043–1047.

Schlingmann, K. P., S. Weber, M. Peters, L. Niemann Nejsum, H. Vitzthum *et al.*, 2002 Hypomagnesemia with secondary hypocalcemia is caused by mutations in TRPM6, a new member of the TRPM gene family. Nat. Genet. **31:** 166–170.

Sulston, J., and J. Hodgkin, 1988 Methods, pp. 587–606 in *The Nematode Caenorhabditis elegans*, edited by W. Wood and the Com-

MUNITY OF *C. ELEGANS* RESEARCHERS. Cold Spring Harbor Laboratory, Cold Spring Harbor, NY.

SUN, A. Y., and E. J. LAMBIE, 1997 *gon-2*, a gene required for gonadogenesis in *Caenorhabditis elegans*. Genetics **147:** 1077–1089.

TAKUWA, N., W. ZHOU and Y. TAKUWA, 1995 Calcium, calmodulin and cell cycle progression. Cell. Signal. **7:** 93–104.

TOMSIG, J. L., and C. E. CREUTZ, 2000 Biochemical characterization of copine: a ubiquitous Ca^{2+}-dependent, phospholipid-binding protein. Biochemistry **39:** 16163–16175.

TREININ, M., and M. CHALFIE, 1995 A mutated acetylcholine receptor subunit causes neuronal degeneration in *C. elegans*. Neuron **14:** 871–877.

WALDER, R. Y., D. LANDAU, P. MEYER, H. SHALEV, M. TSOLIA *et al.*, 2002 Mutation of TRPM6 causes familial hypomagnesemia with secondary hypocalcemia. Nat. Genet. **31:** 171–174.

WEST, R. J., A. Y. SUN, D. L. CHURCH and E. J. LAMBIE, 2001 The *C. elegans gon-2* gene encodes a putative TRP cation channel protein required for mitotic cell cycle progression. Gene **266:** 103–110.

WOLF, F. I., and A. CITTADINI, 1999 Magnesium in cell proliferation and differentiation. Front. Biosci. **4:** D607–D617.

XU, X. Z., F. MOEBIUS, D. L. GILL and C. MONTELL, 2001 Regulation of melastatin, a TRP-related protein, through interaction with a cytoplasmic isoform. Proc. Natl. Acad. Sci. USA **98:** 10692–10697.

Communicating editor: P. ANDERSON